

Supplemental Online Content

Smirnov VM, Nassisi M, Hernandez CS, et al. Retinal phenotype of patients with isolated retinal degeneration due to *CLN3* pathogenic variants in a French retinitis pigmentosa cohort. *JAMA Ophthalmol*. Published online January 28, 2021.
doi:10.1001/jamaophthalmol.2020.6089

eMethods.

eFigure 1. Pedigrees

eFigure 2. qPCR for ex.8_ex.9 del

eFigure 3. Mild forms of *CLN3* isolated retinal degeneration

eFigure 4. Severe forms of *CLN3* isolated retinal degeneration

eFigure 5. Full-field ERG

eFigure 6. BCVA progression

eFigure 7. CIC03517, progression

eFigure 8. CIC00350, progression

eFigure 9. CIC01170, progression

eFigure 10. CIC01169, progression

eFigure 11. CIC01168, progression

eFigure 12. 1037229, progression

eFigure 13. CIC09088, progression

eFigure 14. Battenin

eTable. *CLN3* variants reported both in JNCL and isolated retinal degeneration

eReferences.

This supplementary material has been provided by the authors to give readers additional information about their work.

eMethods.

Genetic analysis. Blood samples from the index cases and, when possible, relatives were collected for genetic research and genomic DNA was extracted as previously reported ¹. These DNA samples were collected within the NeuroSensCol DNA bank, for research in neuroscience (PI: JA Sahel, co-PI I Audo, partner with CHNO des Quinze-Vingts, Inserm and CNRS). Targeted next generation sequencing (NGS) was performed in all but one family in collaboration with an external company (IntegraGen, Evry, France). A large panel of genes (200-300) known or presumed to be associated with retinal dystrophies was used for targeted NGS as previously described ^{2,3}. In a family F1517 (eFigure 1), WES was performed in the trio (proband and parents): exons and flanking exonic regions of DNA samples were captured and investigated with in-solution enrichment methodology (SureSelect Clinical Research Exome, Agilent, Massy, France) as reported previously ^{4(p179)}. Image analysis and base calling were performed with Real Time Analysis software (Illumina). For all subjects of the family, overall WES coverage of the captured regions was 96% and 90.67% for 10x and 25x depth of coverage respectively resulting in a mean sequencing depth of 82x per base. Genetic variation annotations were performed by an in-house pipeline (IntegraGen), and results were provided per sample or family in tabulated text files. Stringent filtering criteria were used to select most likely pathogenic variant(s): only nonsense, missense, splice site variants or small deletions or insertions (InDels) with a minor allelic frequency ≤ 0.005 in Exome Variants Server (EVS, <http://evs.gs.washington.edu/EVS/>), HapMap (<http://hapmap.ncbi.nlm.nih.gov/>), 1000Genomes (<http://www.1000genomes.org/>) and Genome Aggregation Database (GnomAD, <http://gnomad.broadinstitute.org/>) were considered to be putative disease-causing. If never reported, variant pathogenicity was predicted with bioinformatic tools: Polymorphism Phenotyping v.2 (PolyPhen2, <http://genetics.bwh.harvard.edu/pph2/>), Sorting Intolerant From Tolerant (SIFT, <http://sift.jcvi.org/>), MutationTaster (<http://www.mutationtaster.org/>) and

amino acid conservation across species was studied with UCSC Genome Browser (<http://genome.ucsc.edu/index.html>; Human GRCh38/hg38 Assembly).

The *CLN3* variants selected after targeted NGS/WES were validated in the index cases and relatives by Sanger sequencing (refseq: NM_001042432.1, primer sequence available on demand). Quantitative polymerase chain reaction (qPCR) was performed to validate the common ex.8_ex.9 1.02kb deletion detected as a copy number variant (CNV) by NGS/WES (eFigure 2).

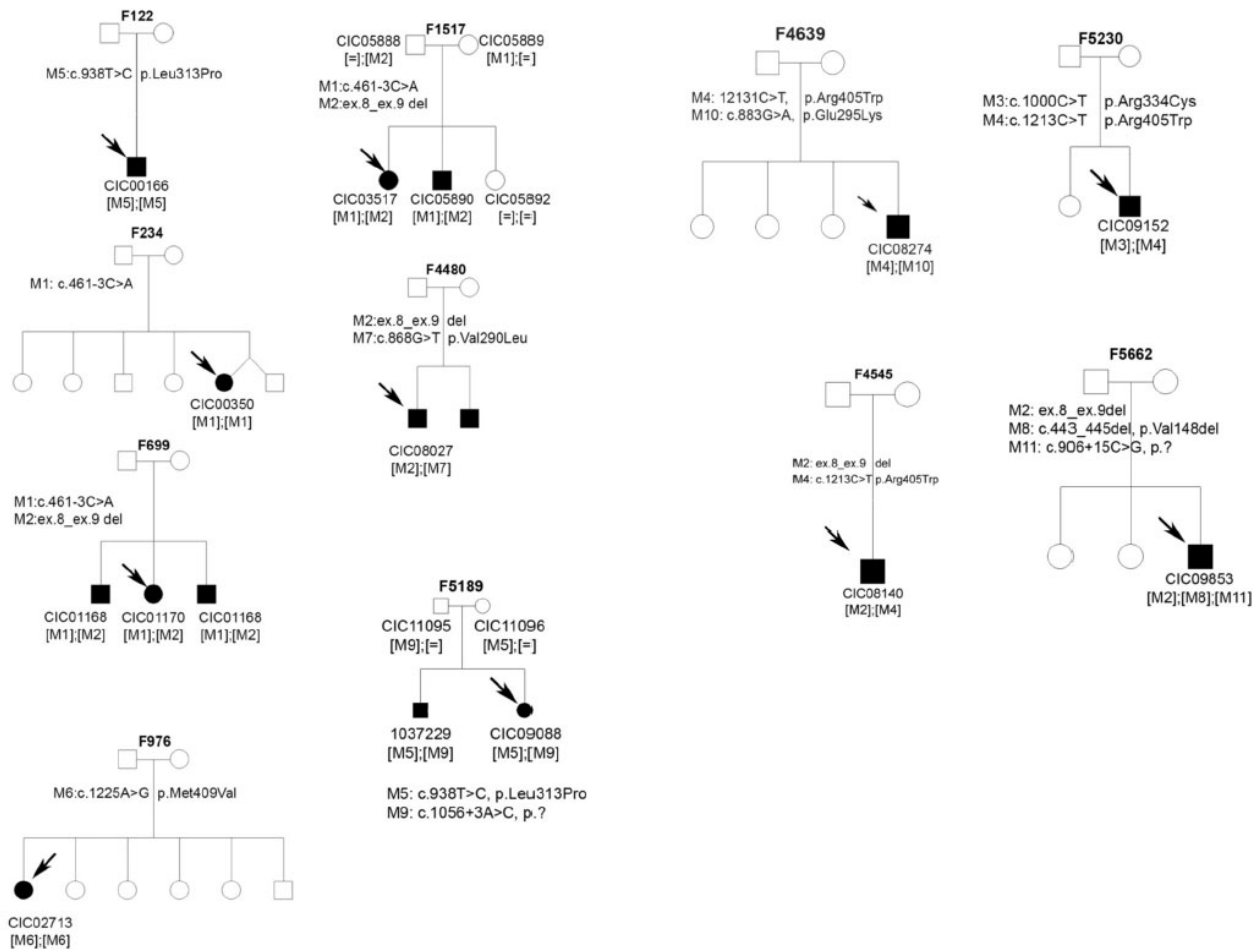
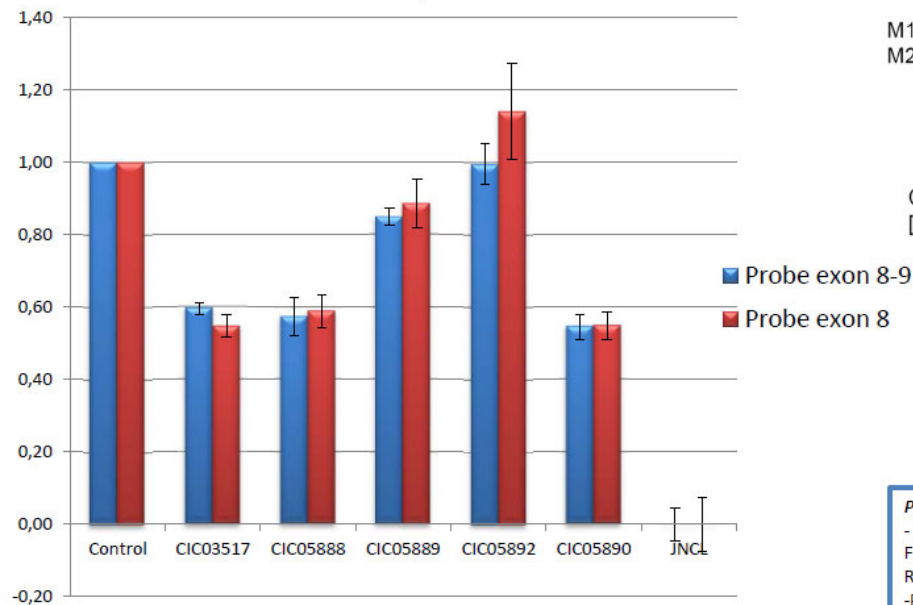
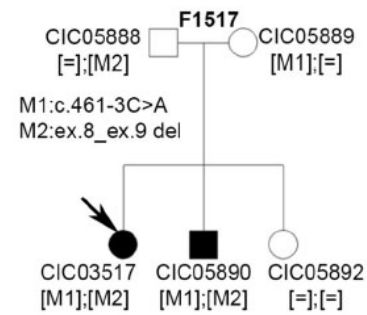


Figure 1. Pedigrees. 15 patients from 11 unrelated families harbored biallelic pathogenic variants in *CLN3*.

Normalized Relative Quantity Exon 8 and 9/Exon10
Family 1517



JNCL: patient homozygous for ex.8_ex.9 1,02kb del, used as negative control

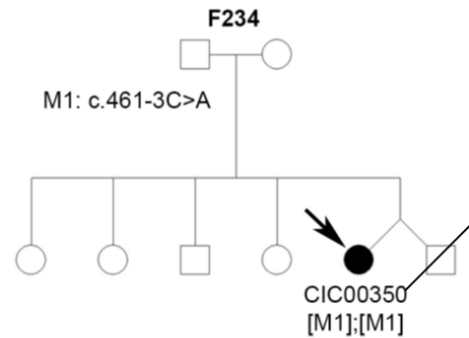
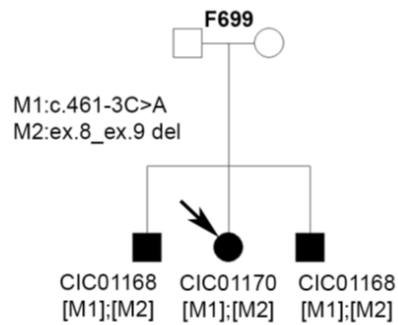
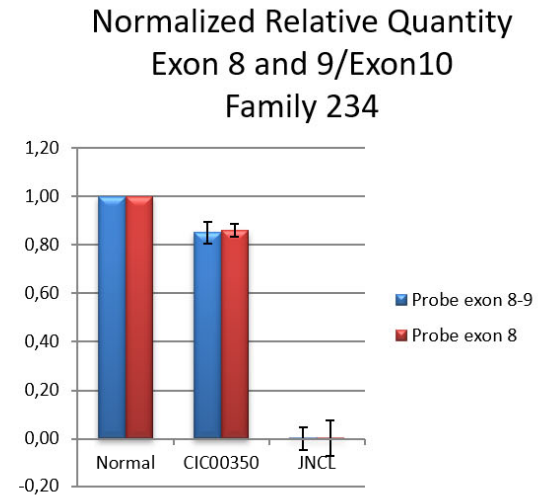
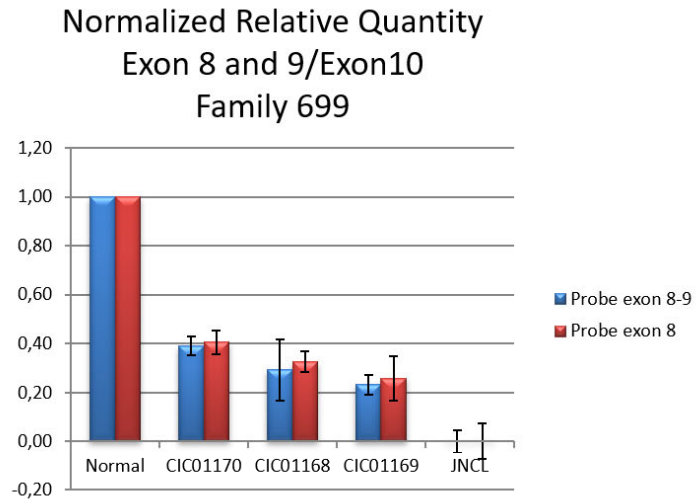


Primers for qPCR SYBR green

- Probe exon 8-9
 - F: TCGCTAGCATCTCATCAGGC
 - R: CCCTGGGAAGGAGAACA 153pb
- Probe exon 8
 - F: GCAGAGACATCAAGGGTGC
 - R: ATGGCCTCCTCAGTATCAGC 170pb
- Probe exon 10
 - F: AGGTAGGAGACACAGACCCT
 - R: CTGTGCTCGTCCTCAACAAG 162pb

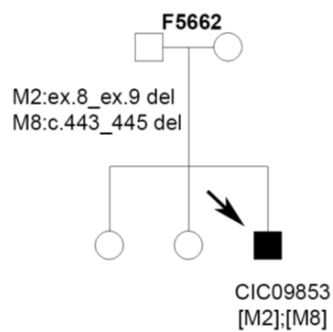
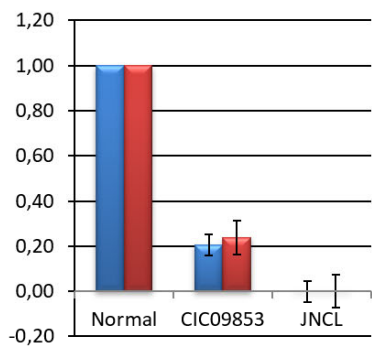
Endogenous control: GAPDH

eFigure 2. qPCR for ex.8_ex.9 del in *CLN3*. Amplification ratios from patients are compared with normal control and with JNCL patient homozygous for ex.8_ex.9 1.02kb del. Patients CIC03517, CIC05888, CIC0589 are heterozygous for this del. Patient CIC05892 have no del.

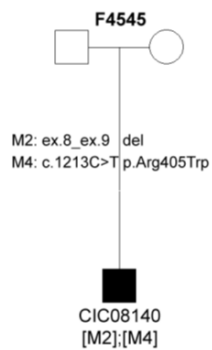
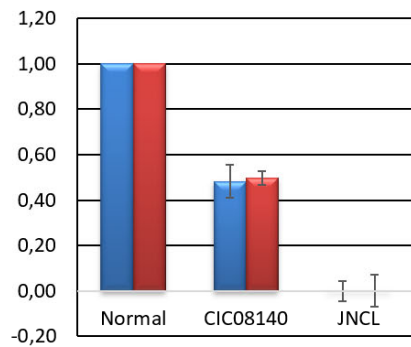


eFigure 2(continued). qPCR for ex.8_ex.9 del in *CLN3*. Patient CIC01168, CIC01169, CIC01170 are heterozygous for the deletion. Patient CIC00350 have no deletion.

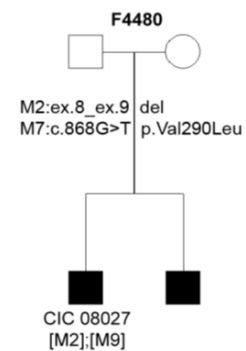
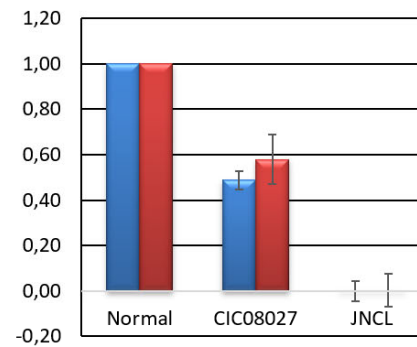
Normalized Relative Quantity
Exon 8 and 9/Exon10
Family 5662



Normalized Relative Quantity
Exon 8 and 9/Exon10
Family 4545



Normalized Relative Quantity
Exon 8 and 9/Exon10
Family 4480



eFigure 2 (end). qPCR for ex.8_ex.9 del in *CLN3*. Patients CIC09853, CIC08140, CIC08027 are heterozygous for the deletion.

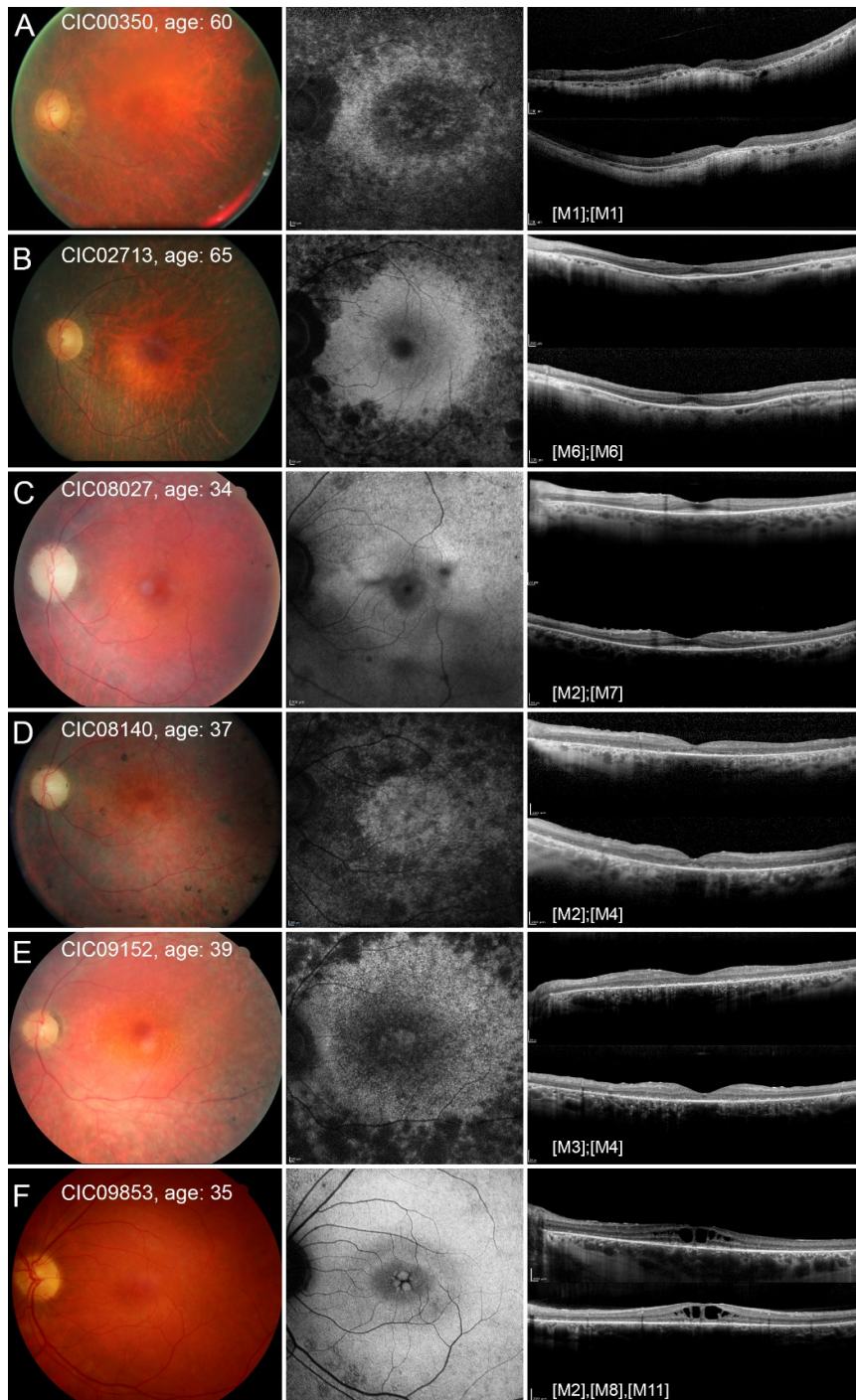
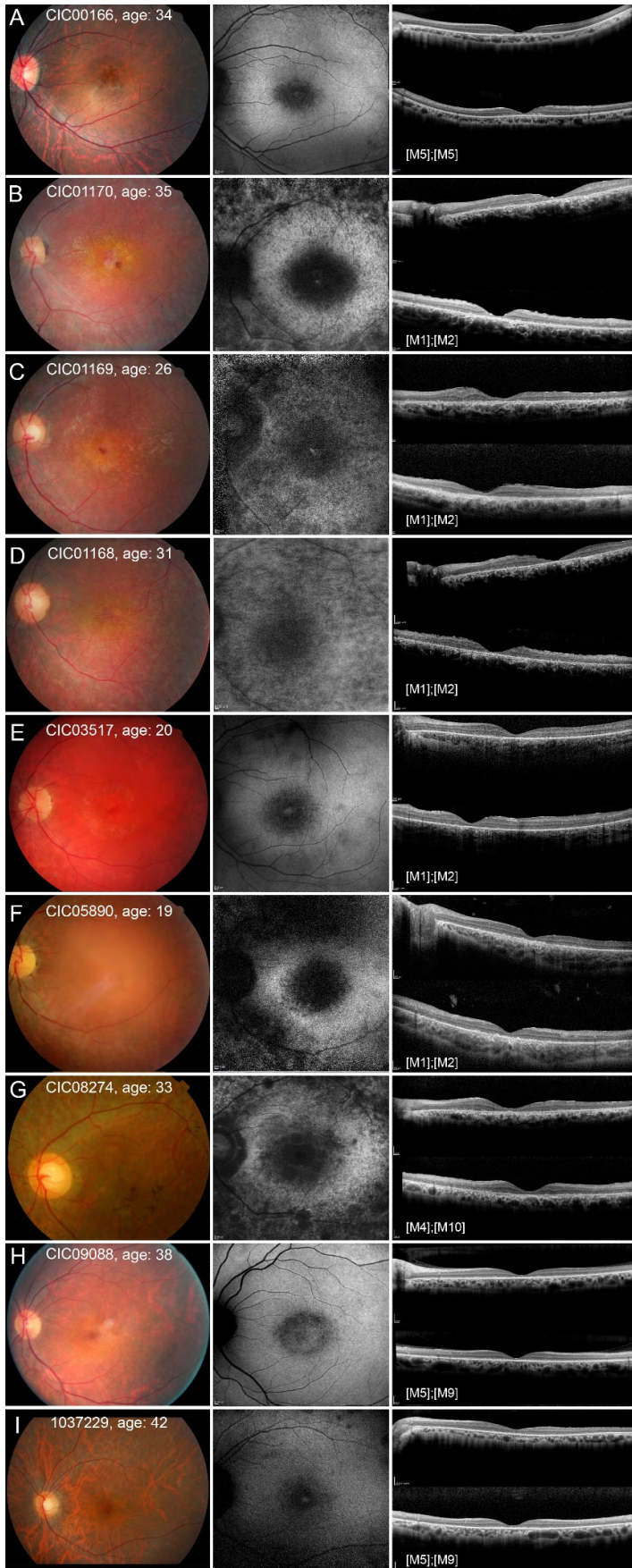
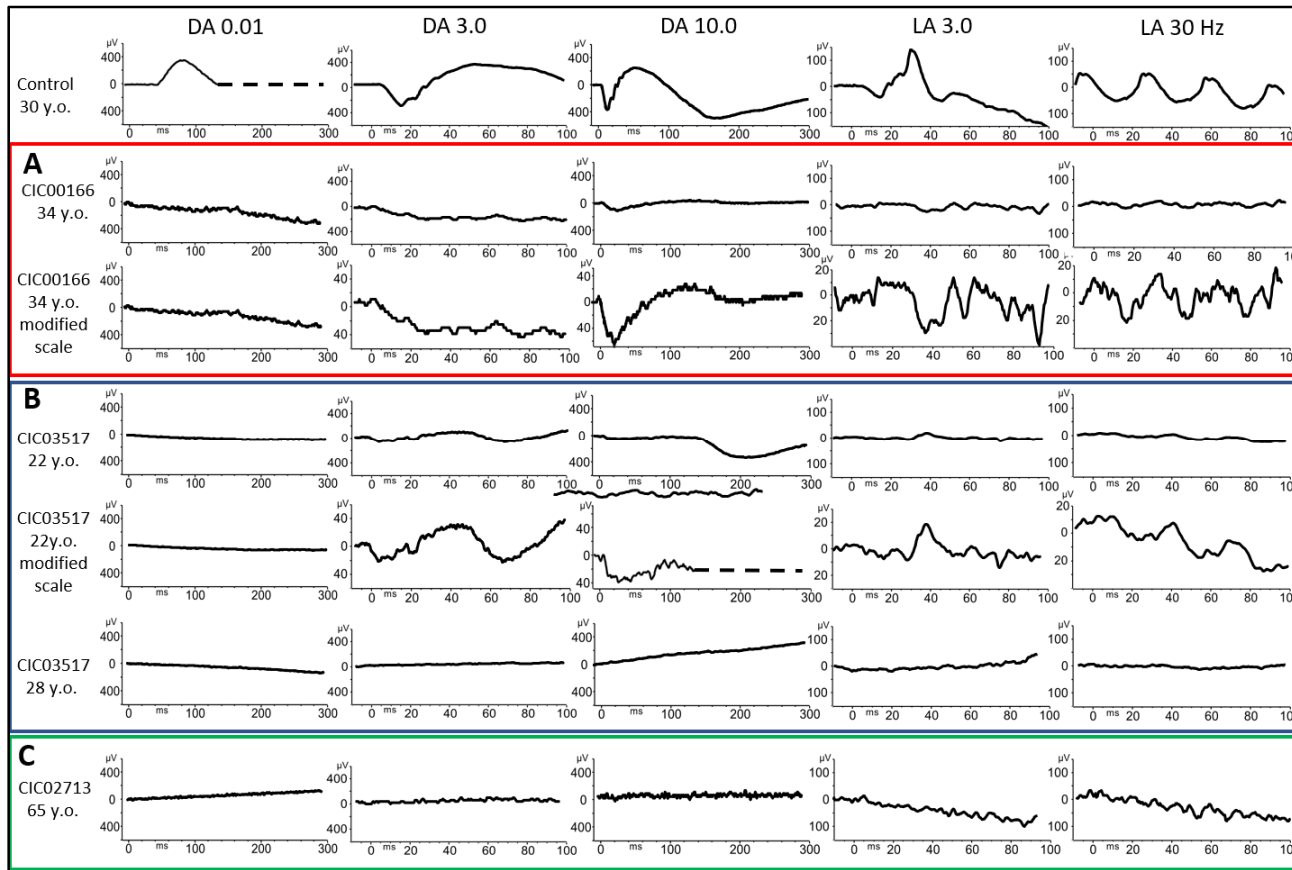


Figure 3. Mild forms of CLN3-isolated retinal degeneration (group A). *Fundus photo, SW-FAF, SD-OCT (Top: horizontal scan, Bottom: vertical scan).* In all cases midperipheral retina is more atrophic than the macular retina. **B**, Vascular narrowing, peripheral greyish discoloration of the retina, pigmentary migrations. Persistence of outer retinal layers in foveal zone on SD-OCT. **C**, Persistence of outer retinal layers in foveal zone on SD-OCT. Changes at the vitreo-retinal interface (striae). **D**, Waxy pallor of the optic disc, vascular attenuation and diffuse pigmentary clumping. Little island of foveal outer retina is preserved on SD-OCT. **E**, more advanced outer retinal degeneration with large ellipsoid zone disruption. **F**, intraretinal microcysts.



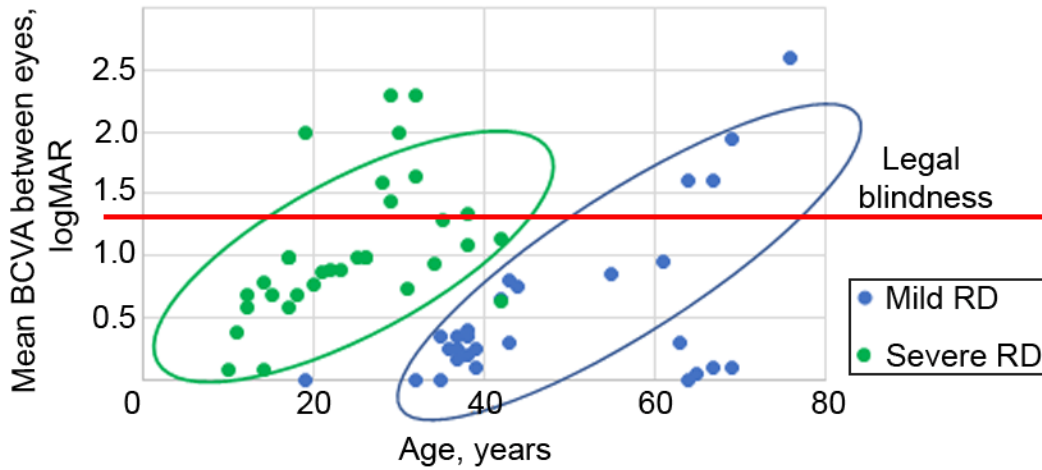
In all cases, atrophic macular changes are prominent. **A**, Only slight macular atrophic changes are seen on fundus photos and SW-FAF. However, SD-OCT reveals a widespread outer retinal layer disruption. **B,C, D**, Family F699, Retinal findings in this family are quite homogenous. Atrophic yellowish maculae with cellophane sheen, arteriolar narrowing and greyish midperipheral retina with sparse pigmentary clumping. Hypo-autofluorescent foveae circled by a broad hyper-autofluorescent ring with indistinct borders on SW-FAF. **E,F**, Family F1517, intrafamilial variability with more a severe retinal disease in CIC05890 at the same age: cataract, obvious macular and midperipheral atrophic retinal changes and waxy optic disc. **G**, Punched-out atrophic macular changes and some macular pigmentary migration as well as midperipheral retinal atrophy. **H,I**, Family F5189. Despite little atrophic macular changes seen on fundus photos and SW-FAF, outer retinal degeneration is more widespread on SD-OCT.

eFigure 4. Severe forms of CLN3 isolated retinal degeneration (group B). Fundus photo, SW-FAF, SD-OCT (Top: horizontal scan, Bottom: vertical scan).

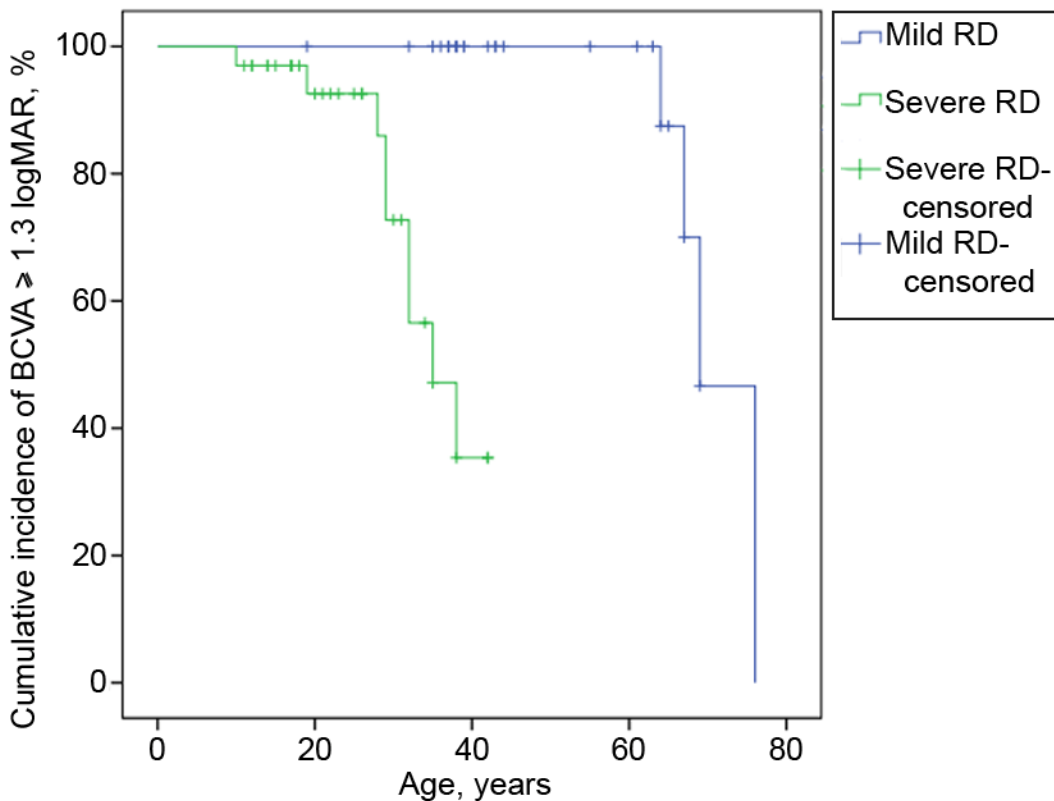


eFigure 5. ISCEV standard full field ERG. A, B: « severe » retinal generation (group B) patients. Undetectable responses to dim dark-adapted flash (DA 0,01). Severely reduced amplitude of the responses to a bright dark-adapted flash (DA 3,0 and DA 10,0) along with reduced b/a ratio, suggesting some degree of inner retinal dysfunction. Severely reduced responses to light-adapted stimulations (LA 3,0 and LA 30 Hz). ERG became undetectable with time. C: « mild » (group A) retinal degeneration patient. DA responses are undetectable. Residual response to the LA 30Hz flicker. Note the age of patient (mild but advanced retinopathy).

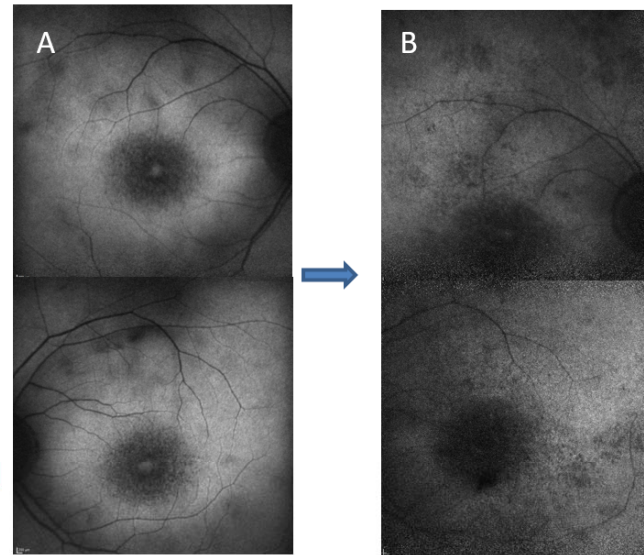
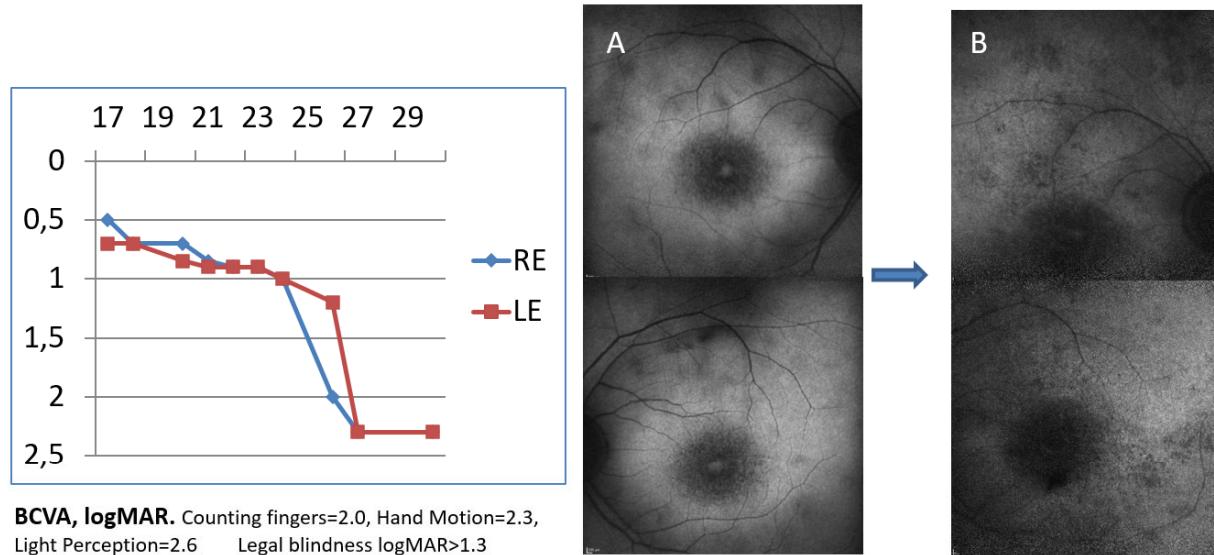
A. Mean BCVA vs age



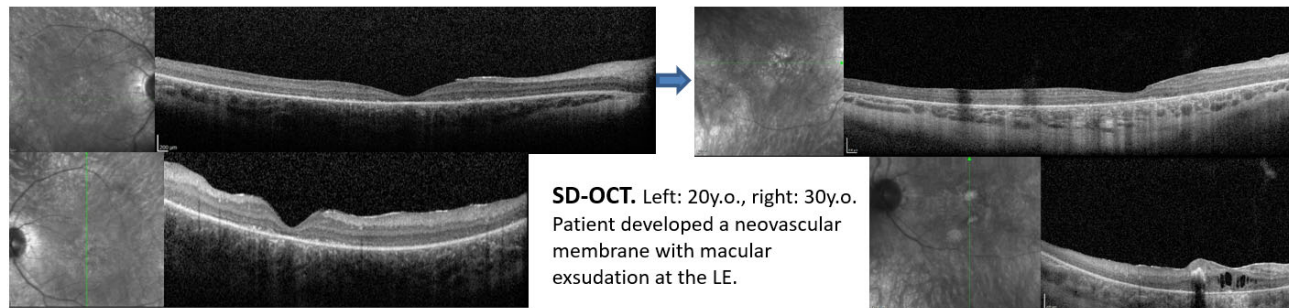
B. Mean BCVA ≥ 1.3 logMAR



eFigure 6. BCVA progression. A, logMAR BCVA vs age. B, Kaplan-Meier analysis for mean BCVA between right and left eye equal or greater than 1.3 logMAR vs. age.

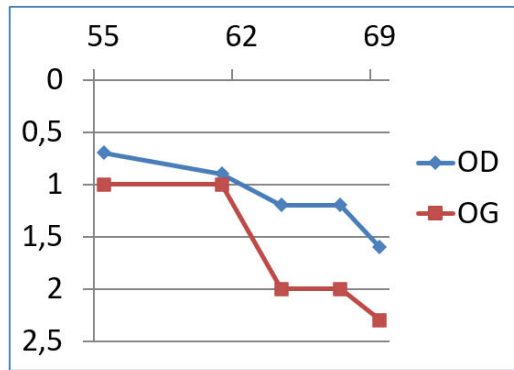


SW-FAF. A: 20 y.o., B: 30y.o. Progression of hypoAF spots.

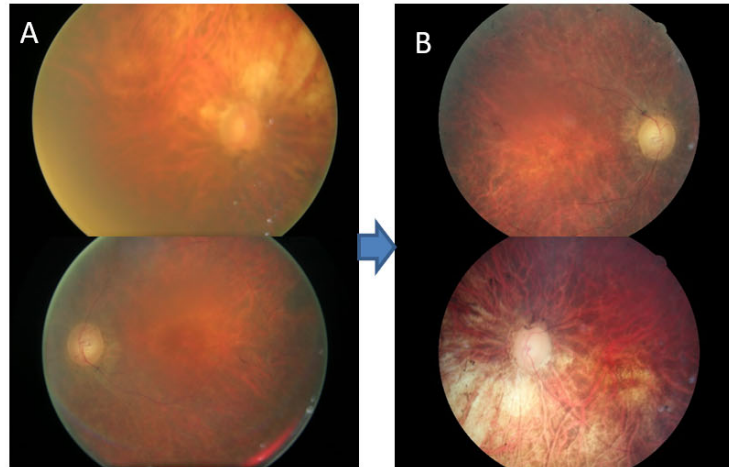


SD-OCT. Left: 20y.o., right: 30y.o. Patient developed a neovascular membrane with macular exudation at the LE.

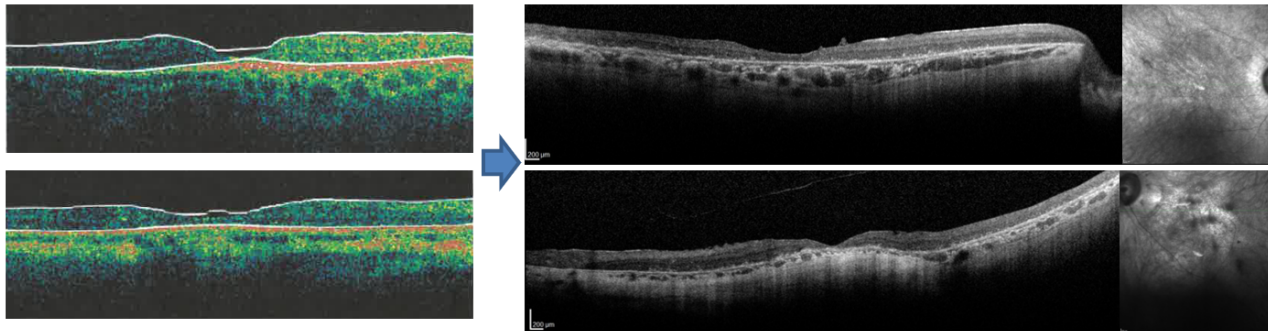
eFigure 7. CIC03517, progression: severe retinal degeneration, macular atrophy. *CLN3*: c.461-3C>G/ex.8_ex.9del 1.02kb



BCVA, logMAR. Counting fingers=2.0, Hand Motion=2.3, Light Perception=2.6; Legal blindness logMAR>1.3

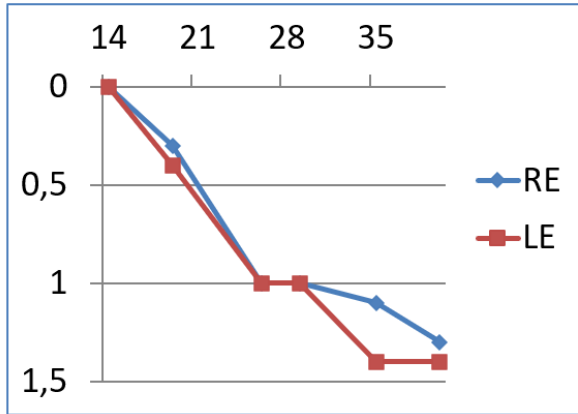


Fundus. Left panel: 60 y.o., right panel: 65 y.o. Cataract surgery performed at 63y.o.

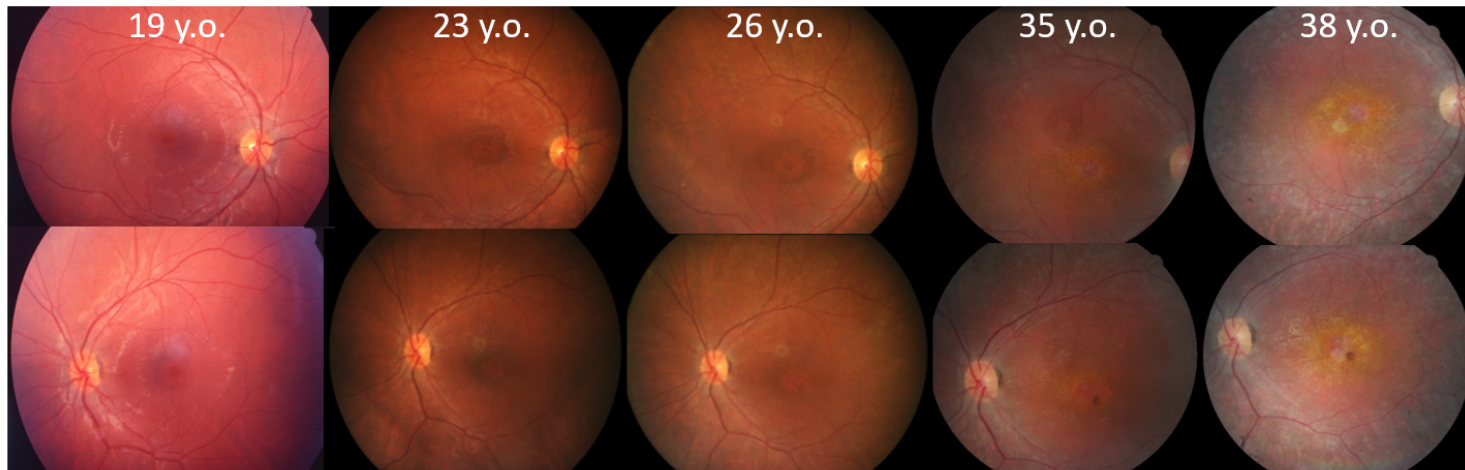
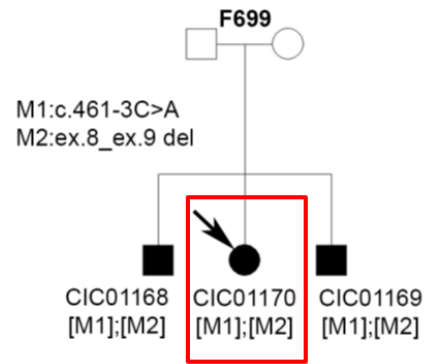


SD-OCT. Left: 60y.o., right: 69y.o.

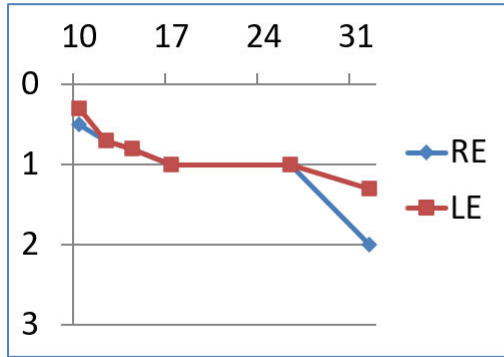
eFigure 8. CIC00350, progression: middle age-onset rod-cone dystrophy. *CLN3*: homozygous c.461-3C>A



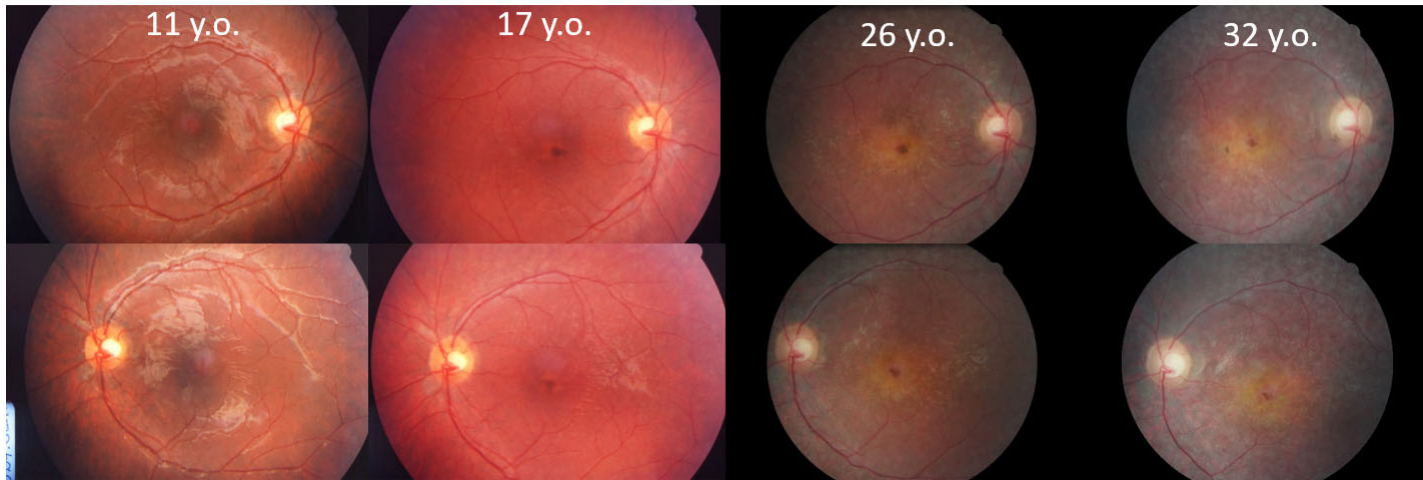
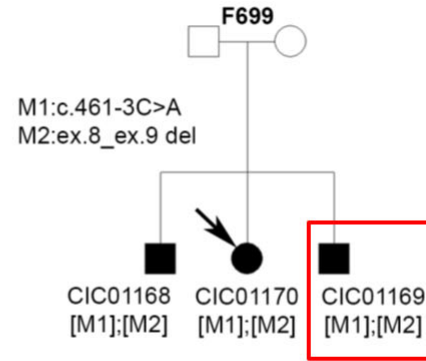
BCVA, logMAR. Counting fingers=2.0, Hand Motion=2.3, Light Perception=2.6. Legal blindness logMAR>1.3



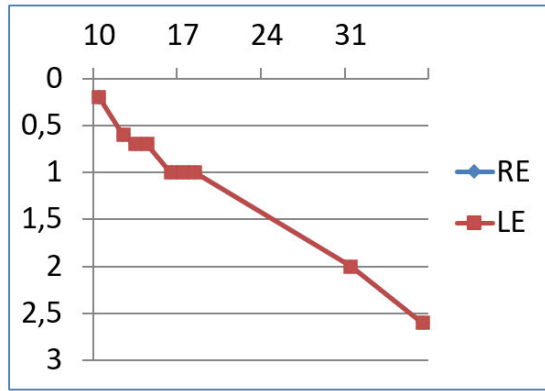
eFigure 9. CIC01170, progression: severe retinal degeneration with early macular atrophy. *CLN3*: M1: c.461-3C>G; M2: ex.8_ex.9del 1.02kb



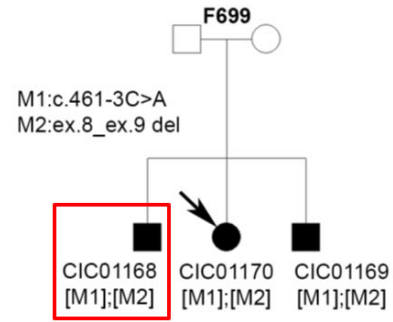
BCVA, logMAR. Counting fingers=2.0, Hand Motion=2.3, Light Perception=2.6 Legal blindness logMAR>1.3



eFigure 10. CIC01169, progression: severe retinal degeneration with early macular atrophy. *CLN3*: c.461-3C>G/ex.8_ex.9del 1.02kb

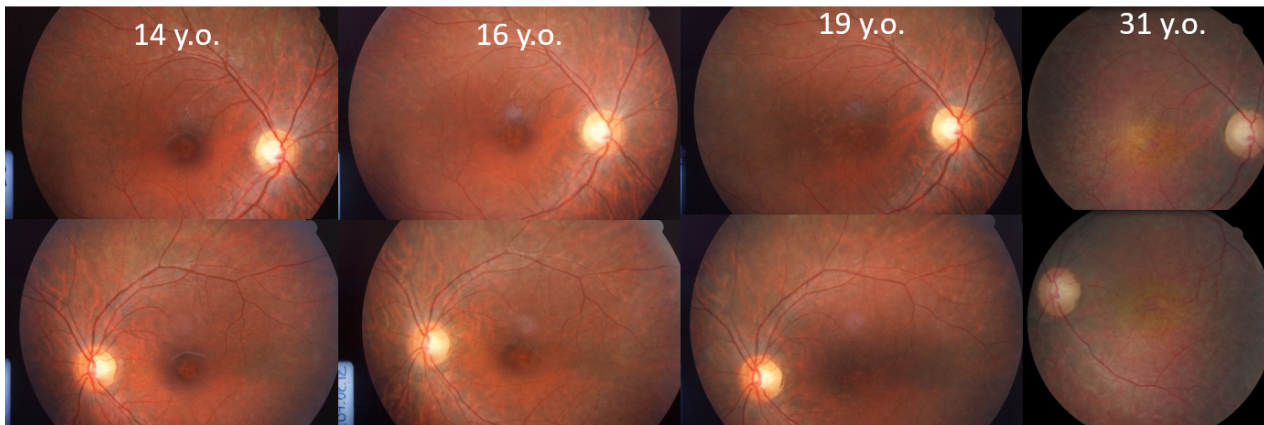


BCVA, logMAR. Counting fingers=2.0, Hand Motion=2.3, Light Perception=2.6 Legal blindness logMAR>1.3

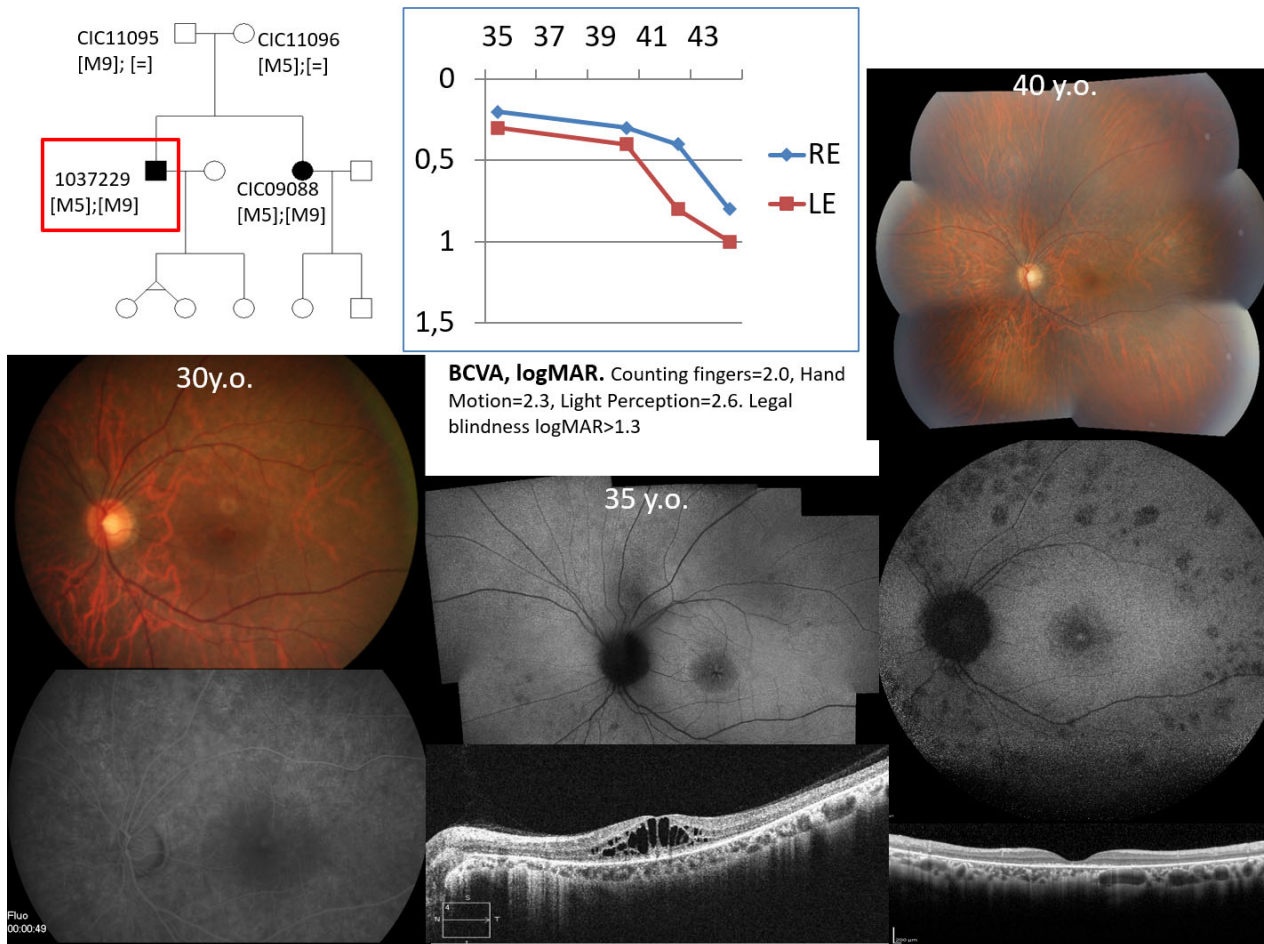


Neuropediatric evaluation at 10 y.o.

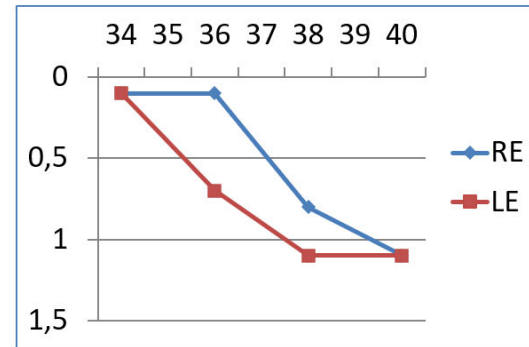
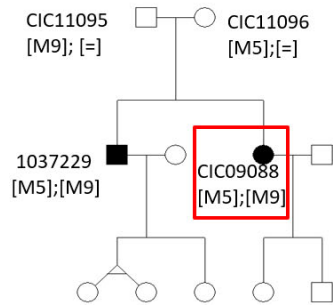
- Neurological examination and psycho-cognitive evaluation were normal
- MRI normal
- Bone marrow analysis normal
- No vacuolated lymphocytes



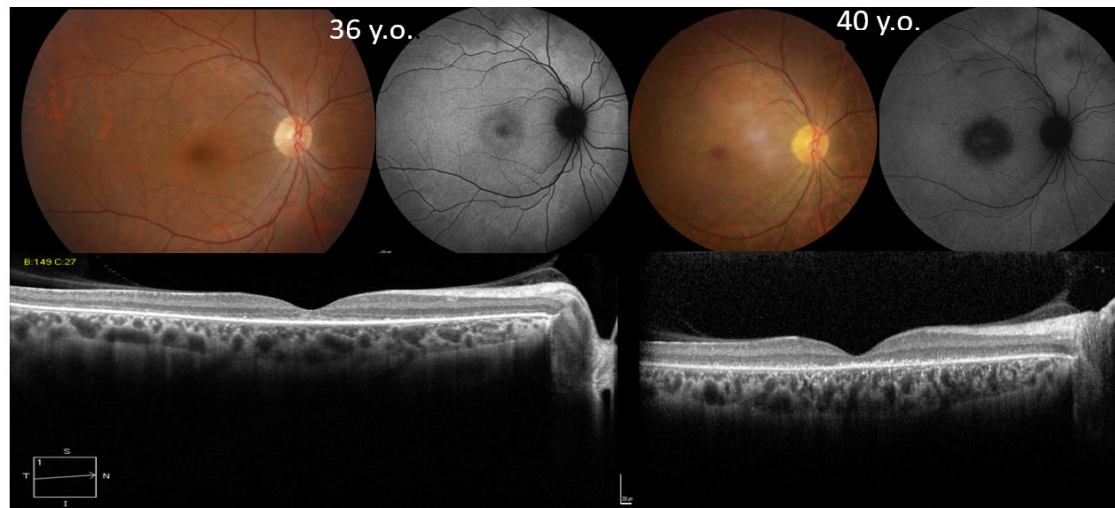
eFigure 11. CIC01168, progression: severe retinal degeneration with early macular atrophy. *CLN3*: c.461-3C>G/ex.8_ex.9del 1,02kb



eFigure 12. Patient 1037229, progression: severe retinal degeneration with early macular atrophy. *CLN3*: M5: c.938T>C p.Leu313Pro; M9: c.1056+3A>C

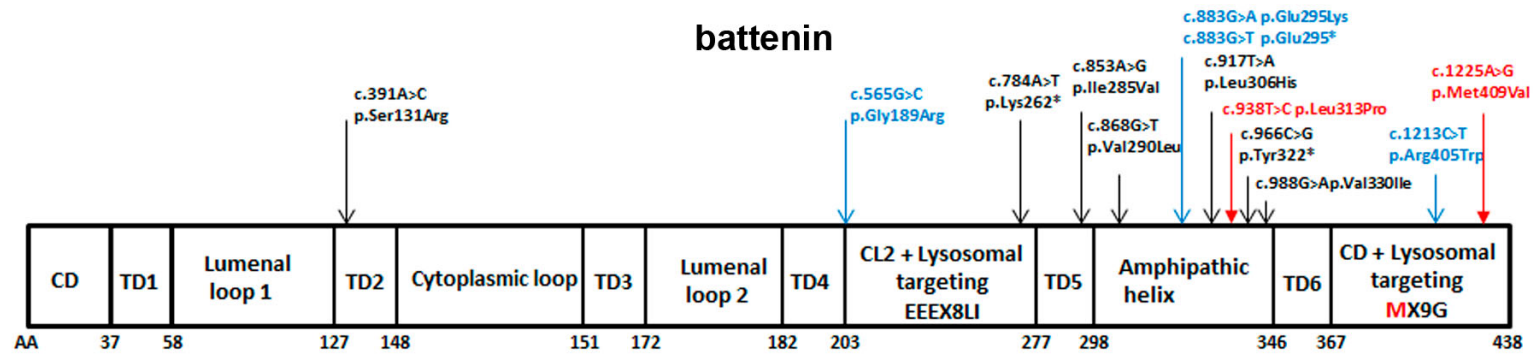


BCVA, logMAR. Counting fingers=2.0, Hand Motion=2.3, Light Perception=2.6. Legal blindness logMAR>1.3



eFigure

13. CIC09088, progression: severe retinal degeneration with early macular atrophy. *CLN3*: M5: c.938T>C p.(Leu313Pro); M9: c.1056+3A>C



eFigure 14. Battenin. Missense and nonsense amino acid changes in battenin, reported in retina-restricted disease. CD, CL: cytoplasmic domain/loop, TD: transmembrane domain. In blue, variants reported in both retina restricted disease and JNCL. In red, novel variants.

eTable. *CLN3* variants reported both in JNCL and isolated retinal degeneration.

JNCL 2 nd allele	Allele detected in both JNCL and non-syndromic IRD	Non-syndromic IRD 2 nd allele
Ex.8_ex.9del 1.02kb ⁵	c.565G>C, p.Gly189Arg ⁵	c.565G>C, p.Gly189Arg ⁶
Ex.8_ex.9del 1.02kb ⁷ Protracted-onset JNCL dominated by visual failure	c.883G>A, p.Glu295Lys ⁷	c.391A>C, p.Ser131Arg ⁶ cone-rod dystrophy
Ex.8_ex.9del 1.02kb ⁸	c.883G>T, p.Glu295* ^{8,9}	c.917T>A, p.Leu306His ¹⁰
<ul style="list-style-type: none"> • c.1247A>G p.Asp416Gly⁵ • ex.2_ex.5del¹¹ 	c.1056+3A>C, p.? ¹²	c.938T>C p.Leu313Pro [this article]

References.

1. Audo I, Lancelot M-E, Mohand-Saïd S, et al. Novel C2orf71 mutations account for ~1% of cases in a large French arRP cohort. *Human Mutation*. 2011;32(4):E2091-E2103. doi:10.1002/humu.21460
2. Boulanger-Scemama E, El Shamieh S, Démontant V, et al. Next-generation sequencing applied to a large French cone and cone-rod dystrophy cohort: mutation spectrum and new genotype-phenotype correlation. *Orphanet J Rare Dis*. 2015;10. doi:10.1186/s13023-015-0300-3
3. Audo I, Bujakowska KM, Léveillard T, et al. Development and application of a next-generation-sequencing (NGS) approach to detect known and novel gene defects underlying retinal diseases. *Orphanet J Rare Dis*. 2012;7:8. doi:10.1186/1750-1172-7-8
4. Audo I, Bujakowska K, Orhan E, et al. Whole-exome sequencing identifies mutations in GPR179 leading to autosomal-recessive complete congenital stationary night blindness. *Am J Hum Genet*. 2012;90(2):321-330. doi:10.1016/j.ajhg.2011.12.007
5. Kousi M, Lehesjoki A-E, Mole SE. Update of the mutation spectrum and clinical correlations of over 360 mutations in eight genes that underlie the neuronal ceroid lipofuscinoses. *Hum Mutat*. 2012;33(1):42-63. doi:10.1002/humu.21624
6. Wang F, Wang H, Tuan H-F, et al. Next generation sequencing-based molecular diagnosis of retinitis pigmentosa: identification of a novel genotype-phenotype correlation and clinical refinements. *Hum Genet*. 2014;133(3):331-345. doi:10.1007/s00439-013-1381-5
7. Munroe PB, Mitchison HM, O'Rawe AM, et al. Spectrum of mutations in the Batten disease gene, CLN3. *Am J Hum Genet*. 1997;61(2):310-316. doi:10.1086/514846
8. Bell CJ, Dinwiddie DL, Miller NA, et al. Carrier Testing for Severe Childhood Recessive Diseases by Next-Generation Sequencing. *Science Translational Medicine*. 2011;3(65):65ra4-65ra4. doi:10.1126/scitranslmed.3001756
9. Zhong N, Moroziewicz DN, Ju W, et al. Heterogeneity of late-infantile neuronal ceroid lipofuscinosis. *Genet Med*. 2000;2(6):312-318. doi:10.1097/00125817-200011000-00002
10. Ku CA, Hull S, Arno G, et al. Detailed Clinical Phenotype and Molecular Genetic Findings in CLN3-Associated Isolated Retinal Degeneration. *JAMA Ophthalmol*. 2017;135(7):749-760. doi:10.1001/jamaophthalmol.2017.1401
11. Wright GA, Georgiou M, Robson AG, et al. Juvenile Batten Disease (CLN3): Detailed Ocular Phenotype, Novel Observations, Delayed Diagnosis, Masquerades, and Prospects for Therapy. *Ophthalmology Retina*. Published online November 2019:S2468653019306293. doi:10.1016/j.oret.2019.11.005
12. Lojewski X, Staropoli JF, Biswas-Legrand S, et al. Human iPSC models of neuronal ceroid lipofuscinosis capture distinct effects of TPP1 and CLN3 mutations on the endocytic pathway. *Hum Mol Genet*. 2014;23(8):2005-2022. doi:10.1093/hmg/ddt596